NASA TECHNICAL MEMORANDUM

NASA TM X-1035

NASA TM X-1035

PRELIMINARY ANALYSIS OF PLASMA-SHEATH ELECTRON DENSITY MEASUREMENTS AT ENTRY VELOCITIES

by William L. Grantham

Langley Research Center
Langley Station, Hampton, Va.

NATIONAL AERONAUTICS AND SPACE ADMINISTRATION • WASHINGTON, D. C. • NOVEMBER 1964

PRELIMINARY ANALYSIS OF PLASMA-SHEATH ELECTRON DENSITY MEASUREMENTS AT ENTRY VELOCITIES

By William L. Grantham

Langley Research Center
Langley Station, Hampton, Va.

NATIONAL AERONAUTICS AND SPACE ADMINISTRATION

PRELIMINARY ANALYSIS OF PLASMA-SHEATH ELECTRON DENSITY MEASUREMENTS AT ENTRY VELOCITIES*

By William L. Grantham
Langley Research Center

SUMMARY

The experimental payload launched from the NASA Wallops Station, April 10, 1964, achieved a maximum velocity of 18,143 ft/sec during the ascending portion of the flight. A three-frequency microwave reflectometer system in the payload measured the plasma-sheath electron density and standoff distance at discrete locations along the RAM (radio attenuation measurement) B3 vehicle. The in-flight diagnostic measurements were made to determine the applicability of various theoretical concepts used for defining reentry plasma characteristics in the velocity region of 10,000 to 20,000 ft/sec.

A heat-sink type of nose cone was used to keep the plasma free of ablation products during the data period. The nose cone of the RAM B3 had a hemispherical 4-inch radius and a 9° half-angle afterbody. A brief description of the reflectometer measurement technique and the results of some ground tests using the reflectometer are given. The in-flight plasma measurements given deviate from approximate calculations in some altitude-velocity regions. This deviation may be due to boundary-layer and finite-rate chemical processes. A detailed judgment of whether theory agrees with the flight data must await finite-rate chemical calculations.

INTRODUCTION

The problem of radio blackout during reentry, caused by free electrons in the flow field of the spacecraft, has been studied for a number of years. (See refs. 1, 2, and 3.) The study of the radio blackout problem can be divided into three main areas: the calculation of plasma parameters (refs. 4, 5, and 6), the interaction of electromagnetic waves with the plasma (refs. 7, 8, and 9), and the alleviation of radio blackout (refs. 10, 11, and 12).

Much information has been obtained about the reentry plasma sheath from ground facilities such as shock tubes and wind tunnels. The interaction of electromagnetic waves with reentry plasmas and methods of eliminating radio blackout have both been studied successfully at the Langley Research Center in a series of rocket flight experiments and ground tests designated Project RAM (radio attenuation measurements). (See refs. 10 to 13.) The RAM B3 flight

*Title, Unclassified.

experiment was designed specifically to study plasma parameters in an effort to understand reentry plasma physics better and to improve the calculations of radio blackout times. In particular, the RAM B3 experiment was designed to measure in-flight plasma parameters in the velocity region of 10,000 to 20,000 ft/sec by using microwave reflectometers operating in the L-, S-, and X-bands.

The microwave reflectometer measurement technique used to determine the flight plasma-electron density utilized the reflective nature of the plasma. This technique, or methods similar to it, has been used for plasma diagnosis of laboratory plasmas for some time. (See refs. 14 to 17.) Since the reflectometer technique is based on the well-known interaction theory of electromagnetic waves and plasmas, only the application of the interaction for measuring electron density will be discussed.

SYMBOLS

f	frequency, cps
N_e	electron density per cubic centimeter
X/D	body station normalized to nose diameter
l	distance along transmission path, cm
ρ	power reflection coefficient

Subscripts:

cr	critical
1,2,3	frequency for L-, S-, and X-bands, respectively

DESCRIPTION OF APPARATUS

Vehicle

The RAM B3 booster vehicle consisted of a Castor motor as the first stage, an Antares motor as the second stage, and an Alcor motor as the third stage. The payload nose cone had a hemispherical 4-inch radius nose with a 9° half-angle afterbody and was made of beryllium for heat protection and for minimum contamination of the flow field. A spin of about 3 revolutions per second obtained with two spin motors and canted fins stabilized the vehicle. The angle of attack of the vehicle was kept below 5° during flight. Figure 1 is a drawing of the vehicle.

Reflectometer System

A block diagram is shown in figure 2 of the L-, S-, and X-band flight systems. The L- and S-band systems are schematically identical. The basic measurements are forward power, reflected power, and probe voltages in the main transmission line. Antenna locations used in flight are shown in figure 3. Two antennas are used for each microwave frequency. A coaxial switch alternately transfers the microwave power from one antenna to the other in order to increase the number of data points available from each frequency used.

The S- and X-band antennas located on the forward portion of the vehicle were open-ended circular waveguides with half-wavelength quartz windows. (See fig. 4.) The quartz windows reached a temperature of about 2500° F during the flight. Qualification tests have shown these antennas to function properly under high temperatures. The L-band antennas were T-fed slots and were covered with a protective dielectric.

EXPERIMENTAL METHODS

During the ascending portion of the flight, the flow-field electron density increased to a maximum value and then decreased to zero as the vehicle exited from the earth's atmosphere. A microwave reflectometer system was used to monitor the occurrence and decay of the critical electron density for the L-, S-, and X-band microwave frequencies used. For a given microwave frequency the critical electron density is given by the equation

$$N_{e,cr} \approx \frac{f^2}{10^8} \frac{\text{electrons}}{\text{cm}^3}$$

The principle of the reflectometer measurements technique can be seen in figure 5. The reflectometer measures the amount of power reflected by the plasma. The plot of the variation of power reflection coefficient with plasma-electron density indicates by the sharp increase in reflection when the plasma-electron density exceeds critical density. The wave transmitted to the plasma is totally reflected only if its critical electron density exists in the plasma. This type of wave-plasma interaction is typical when the electron collision frequency is low.

The use of the reflectometer principle for measuring in-flight plasma-electron densities can be seen in figure 6. At the top of the figure is shown a typical peak electron-density time history for a given body station. The plasma reflection coefficient is measured as a function of time of flight. When reflection occurs, the maximum electron density in the flow field at that body station equals the critical density of the electromagnetic frequency used. When reflection decreases sharply, critical density has decayed at that body station. The times of onset and decay of reflection are the data points and are governed primarily by the electron density in the flow field. Other factors which affect the time of onset and decay of reflection are the plasma thickness,

the electron-molecule collision frequency, and the electron-density gradients. The experiment was designed so that parameters other than electron density do not seriously affect the accuracy of the measurement; that is, the microwave frequencies used for the flight experiment were such that errors due to plasma thickness and collision frequency were minimized. Strong electron-density gradients were expected to exist along the RAM vehicle and thus across the reflectometer antennas. Particular attention was therefore given to the design of the antennas so that electron densities could be measured over small areas along which longitudinal variations of plasma characteristics would be negligible. The antennas used were open-ended waveguides operating in the TE_{11} mode (TE_{10} mode for L-band), which locates the peak energy in the center of the aperture (ref. 18), and the electric field of the antennas was oriented normal to the body axis. The combination of mode and field direction used gave the antenna high resolution ability and thus minimized the measurement errors due to gradients along the body. A preliminary error analysis indicates that ±30-percent error in the electron-density measurement should be typical of the flight data.

The reflectometer antennas were located such that they monitored plasma-electron density under two different gas conditions: First, near stagnation ($X/D = 0.1475$) where at low altitudes the values of electron density can be calculated within close limits (uncertainties due to chemical kinetics are not large at low altitudes) and therefore, agreement is expected between measured and calculated values; second, on the RAM afterbody ($X/D = 0.6, 3.4, 4.5$) where the influence of finite reaction rates is much stronger. At the higher altitudes nonequilibrium would be expected to predominate throughout the flow. Measurements made under these conditions should allow thorough evaluation of various theoretical approaches used for defining the plasma characteristics.

The phase of the reflected wave was monitored during flight, with nondirectional probes to determine the distance from the vehicle surface to the critical-density boundary. The phase of the reflected wave is partly determined by the distance between the vehicle surface and the critical-density boundary. The principle of this measurement is shown in figure 7. If the reflecting boundary (critical-density boundary) moves a distance Δl with respect to the transmitting antenna, the standing wave envelope shifts the same amount. With proper calibration, the voltage change at either of the sampling probes would indicate the standoff distance of the reflecting boundary. The position of the probes with respect to the standing-wave-envelope null determines their rate of voltage change with respect to the reflector distance and, thus, determines the accuracy of the measurement. Two probes are employed one-quarter wavelength apart so that, at any time, one of the two probes will be in an accurate measurement region. Phase measurements were made during flight with the L- and S-band systems and have not yet been fully analyzed.

The reflectometer principle discussed earlier assumes the plasma to be in the far field of the transmitting antenna. During flight, however, the plasma was in the near field of the reflectometer antennas. It was therefore necessary to qualify the flight antennas by determining whether near-field plasma measurements would agree with far-field theoretical values. Two tests were made to qualify the antennas. First, a series of rocket-exhaust plasma measurements,

using a flight type of reflectometer system, were made in the 41-foot-diameter vacuum sphere at the Langley Research Center. The reflectometer system was packaged into a nose cone with a 1-inch radius nose and a 9° half-angle afterbody. (See fig. 8.) A trolley was used to move the rocket motor so that its ionized exhaust plume would periodically engulf the reflectometer model. The rocket-exhaust test simulates the near-field measurement conditions of flight. The results of three rocket-exhaust tests showed good repeatability of the plasma and agreement between the calculated (ref. 19) and measured electron density within a factor of two. Transmission signal-loss measurements were also made during the reflectometer tests and the results agree with the reflectometer measurements. The second near-field qualification test was made by placing thin dielectric slabs (plasma simulators) over the antennas and comparing the near-field reflection coefficient with the calculated far-field coefficient. Similar qualification tests were made in reference 16. The calculated and measured reflection coefficients agreed very well, and the results of the test at X-band are shown in figure 9. The close agreement of far-field calculation and near-field measurements indicates that the far-field theory can be used to interpret the near-field flight measurements.

RESULTS AND DISCUSSION

The ascending flight trajectory achieved by the RAM reflectometer payload is shown in figure 10. An altitude time history is shown in figure 11. For preliminary comparison of the diagnostic data some approximate plasma calculations were made to show the trend of flight data; in particular, inviscid flow field calculations have been made at the four reflectometer antenna locations by using the RAM flight trajectory. The calculations were made for two gas conditions: equilibrium flow and frozen flow (gas constituents are frozen at stagnation and allowed to expand to the aft region). The method used to evaluate the flow field is the same as that used in reference 20 with the exception that the local body-pressure coefficients dictate the scaling factor rather than ambient-pressure coefficients. It would be necessary, however, to make finite-rate calculations before quantitative comparisons or conclusive deductions can be made. Plasma-sheath calculations of peak electron density in the flow field are shown with the reflectometer flight measurements in figures 12.

When the theoretical electron densities given in figures 12 are compared with the in-flight measurements, it is important to keep in mind that:

(1) The calculations are for inviscid flow (no boundary layer) and are for two gas conditions: equilibrium and frozen flow.

(2) The measured electron densities near stagnation should correspond most closely with equilibrium values except at very high altitudes where there may not be sufficient gas collisions to establish equilibrium conditions.

(3) Electron concentrations in the aft portion of the flow field are, in part, governed by the actual concentration at stagnation; therefore, before any analysis can be applied to the aft body electron-density measurements the calculations and measurements should agree near the stagnation region.

In figure 12(a), the greatest discrepancy between measured and calculated electron densities is seen to be at the high-altitude point of 202 seconds. The measured electron density at that time was a factor of about four below the calculated equilibrium value. A detailed judgment of whether theory agrees with the data points given in figures 12 must await calculations which include boundary-layer and finite-rate chemical effects.

CONCLUDING REMARKS

A plasma diagnostic flight experiment has been conducted to determine the applicability of various theoretical concepts used in defining reentry plasma-sheath characteristics. Microwave reflectometer techniques were used during the flight to measure the flow-field electron density. The electromagnetic frequencies used for the diagnostic experiment were at L-, S-, and X-bands and all frequencies were reflected by the plasma sheath during the data period. The comparison of flight data with calculations based on approximate plasma-sheath models indicates that a more comprehensive theoretical approach is required. A more detailed judgment of whether theory agrees with the flight data must await calculations which include boundary-layer and finite-rate chemical effects.

Langley Research Center,
National Aeronautics and Space Administration,
Langley Station, Hampton, Va., August 4, 1964.

REFERENCES

1. Graves, George B., Jr.; and Markley, J. Thomas: Telemeter Transmission at 219.5 Megacycles From Two Rocket-Powered Models at Mach Numbers up to 15.7. NACA RM L58D18a, 1958.

2. Drummond, James E.: Plasma Physics. McGraw-Hill Book Co., Inc., 1961.

3. Lin, S. C.: A Rough Estimate of the Attenuation of Telemetering Signals Through the Ionized Gas Envelope Around a Typical Re-Entry Missile. Res. Rept. 74 (Contract No. AF 04(645)-18), Avco-Everett Res. Lab., Feb. 1956.

4. FitzGibbon, Sheila A.: Real Gas Supersonic Flow Field Solutions in the Shock Layer Around a 9° Sphere-Cone at Mach = 20.4, 21.4, and 21.2. Aerodyn. Data Mem. No. 1:48, Missile and Space Vehicle Dept., Gen. Elec. Co., May 1961.

5. Lin, S. C.; and Teare, J. D.: A Streamtube Approximation for Calculation of Reaction Rates in the Inviscid Flow Field of Hypersonic Objects. Res. Note 223 (AFBSD-TN-61-24), Avco-Everett Res. Lab., Aug. 1961.

6. Eschenroeder, Alan Q.: Ionization Nonequilibrium in Expanding Flows. ARS J., vol. 32, no. 2, Feb. 1962, pp. 196-203.

7. Klein, M. M.; Greyber, H. D.; King, J. I. F.; and Brueckner, K. A.: Interaction of a Non-Uniform Plasma With Microwave Radiation. Planetary Space Sci., vol. 6, 1961, pp. 105-115.

8. Graf, K. A.; and Bachynski, M. P.: Existing Solutions for Interaction of Electromagnetic Waves With Plasma of Simple Geometrics. DAMP Tech. Monograph No. 62-07 (Contract DA 36-034-ORD-3144RD), Radio Corp. Am., June 1962.

9. Swift, Calvin T.; and Evans, John S.: Generalized Treatment of Plane Electromagnetic Waves Passing Through an Isotropic Inhomogeneous Plasma Slab at Arbitrary Angles of Incidence. NASA TR R-172, 1963.

10. Sims, Theo E.; and Jones, Robert F.: Flight Measurements of VHF Signal Attenuation and Antenna Impedance for the RAM A1 Slender Probe at Velocities up to 17,800 Feet per Second. NASA TM X-760, 1963.

11. Russo, F. P.; and Hughes, J. K.: Measurements of the Effects of Static Magnetic Fields on VHF Transmission in Ionized Flow Fields. NASA TM X-907, 1964.

12. Huber, Paul W.; and Nelson, Clifford H.: Plasma Frequency and Radio Attenuation. Proceedings of the NASA-University Conference on the Science and Technology of Space Exploration, Vol. 2, NASA SP-11, 1962, pp. 347-360.

13. Cuddihy, William F.; Beckwith, Ivan E.; and Schroeder, Lyle C.: RAM B2 Flight Test of a Method for Reducing Radio Attenuation During Hypersonic Reentry. NASA TM X-902, 1963.

14. Anisimov, A. I.; Vinogradov, N. I.; Golant, V. E.; and Konstantinov, B. P.: Method of Investigating Electron Spatial Distribution in a Plasma. Soviet Phys. - Tech. Phys., vol. 5, no. 9, Mar. 1961, pp. 939-947.

15. Golant, V. E.: Microwave Plasma Diagnostic Techniques. Soviet Phys. - Tech. Phys., vol. 5, no. 11, May 1961, pp. 1197-1310.

16. Lin, Shao-Chi; Neal, Richard A.; and Fyfe, Walter I.: Rate of Ionization Behind Shock Waves in Air. I. Experimental Results. Phys. of Fluids, vol. 5, no. 12, Dec. 1962.

17. Wharton, Charles B.; and Slager, Donald M.: Microwave Interferometer Measurements for the Determination of Plasma Density Profiles in Controlled Fusion Experiments. UCRL-5400 (Contract No. W-7405-eng-48), Los Alamos Sci. Lab., Univ. of California, Nov. 6, 1958.

18. Southworth, George C.: Principles and Applications of Waveguide Transmission. D. Van Nostrand Co., Inc., c.1950.

19. Cuddihy, W. F., and Hughes, J. Kenrick: Simulated Reentry Tests of a Method for Reducing Radio Blackout by Material Addition to Ionized Flow Field. NASA TM X-988, 1964.

20. Huber, Paul W.: Hypersonic Shock-Heated Flow Parameters for Velocities to 46,000 Feet per Second and Altitudes to 323,000 Feet. NASA TR R-163, 1963.

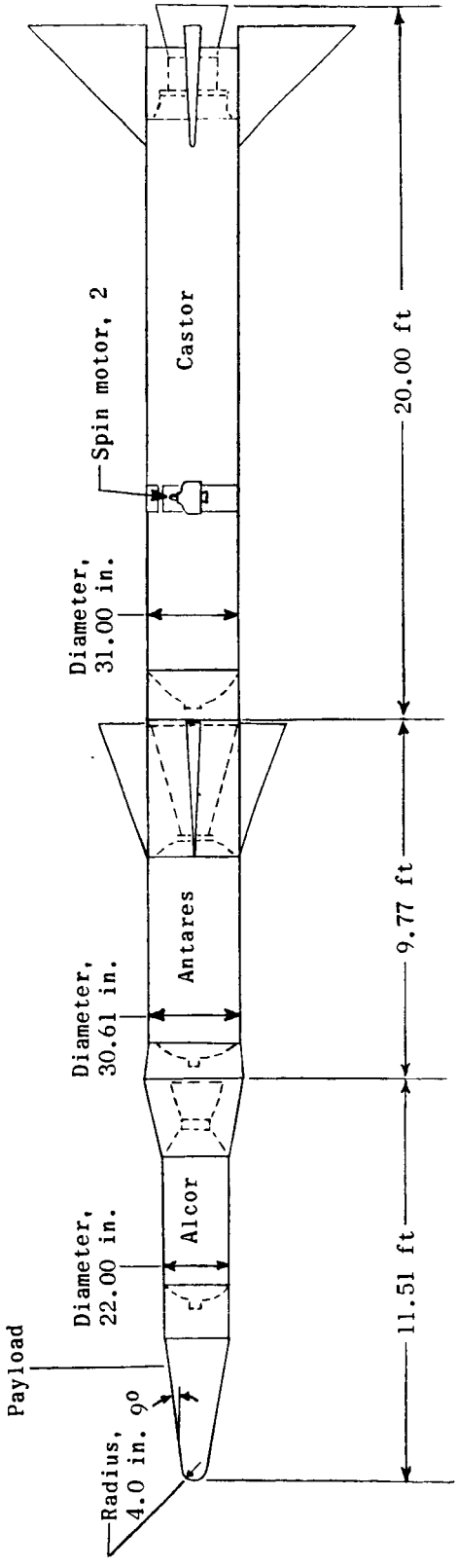

Figure 1.- RAM B3 launch vehicle.

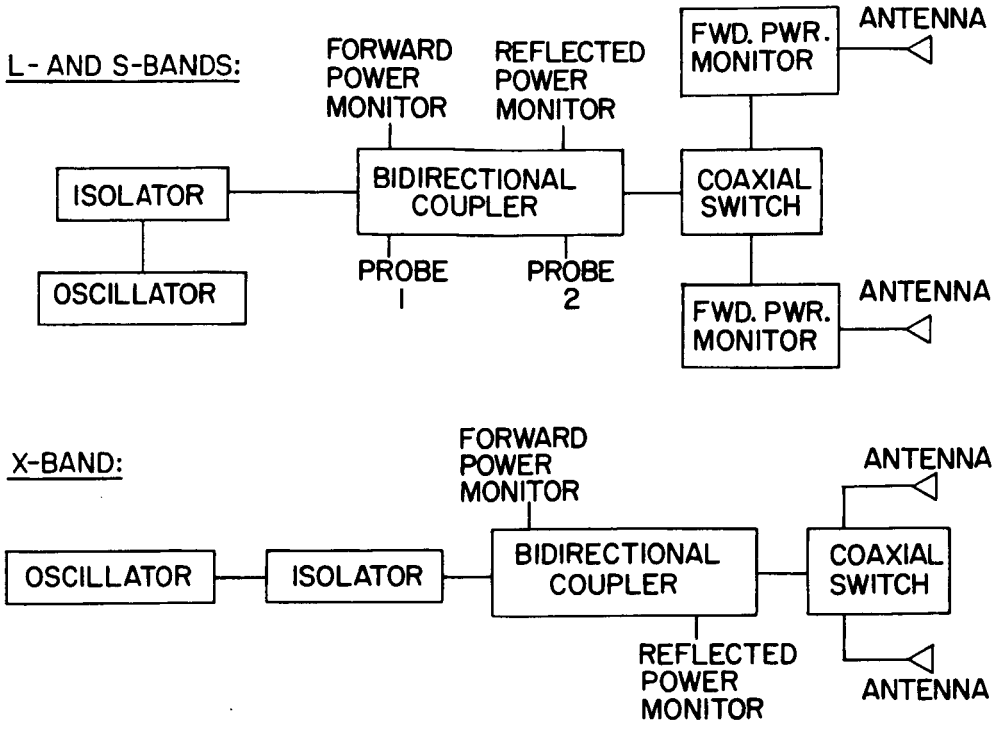

Figure 2.- Reflectometer flight system.

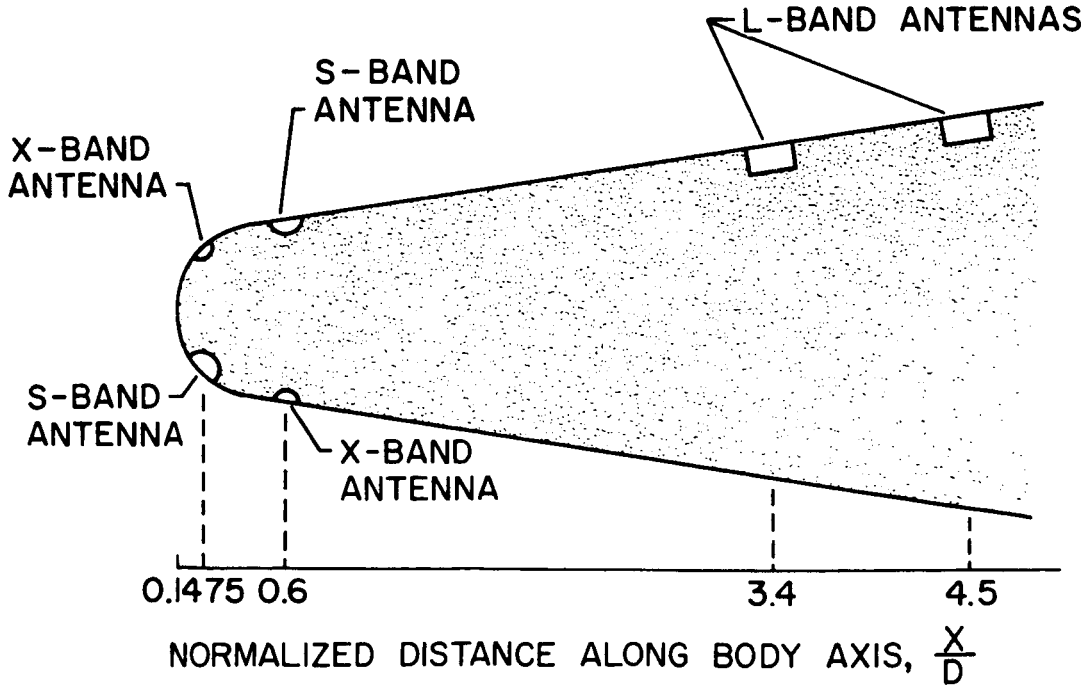

Figure 3.- Reflectometer antenna locations.

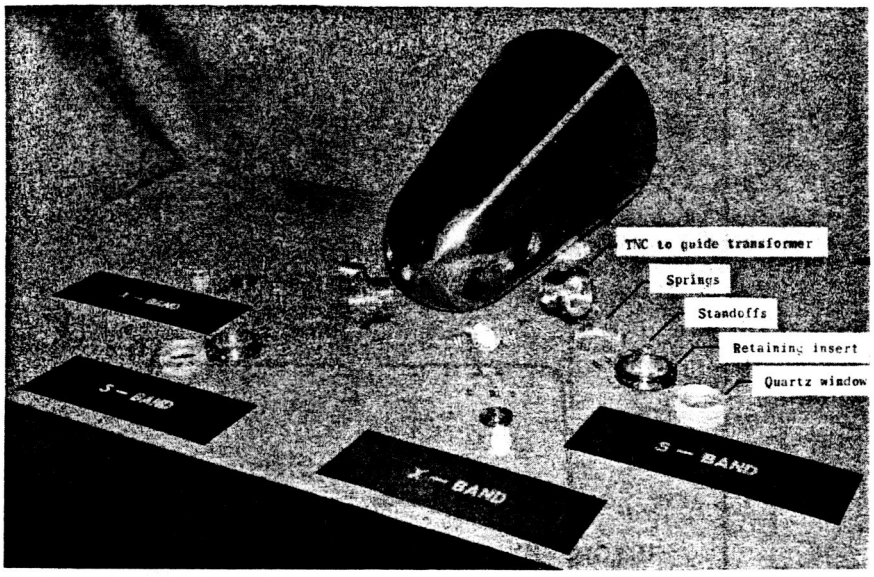

Figure 4.- S-band and X-band flight antenna assemblies. L-63-5157.1

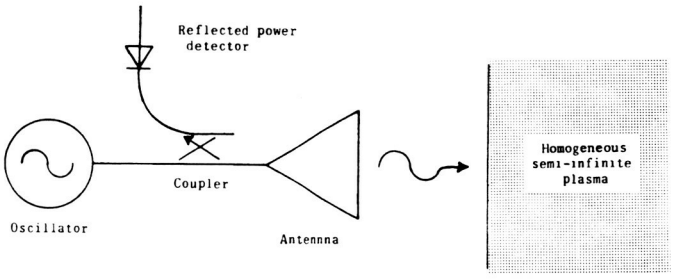

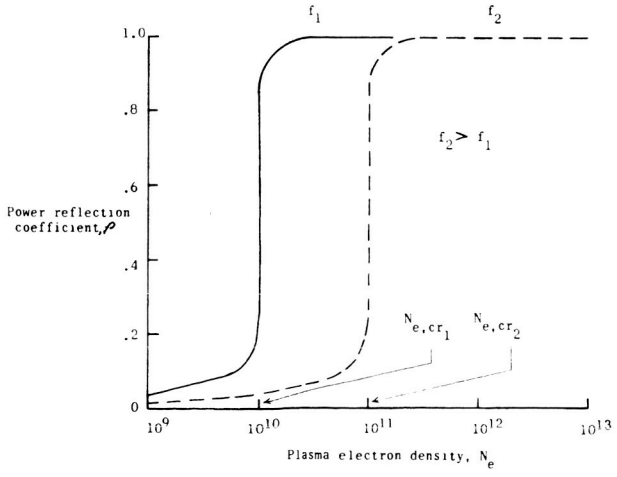

Figure 5.- Reflectometer principle.

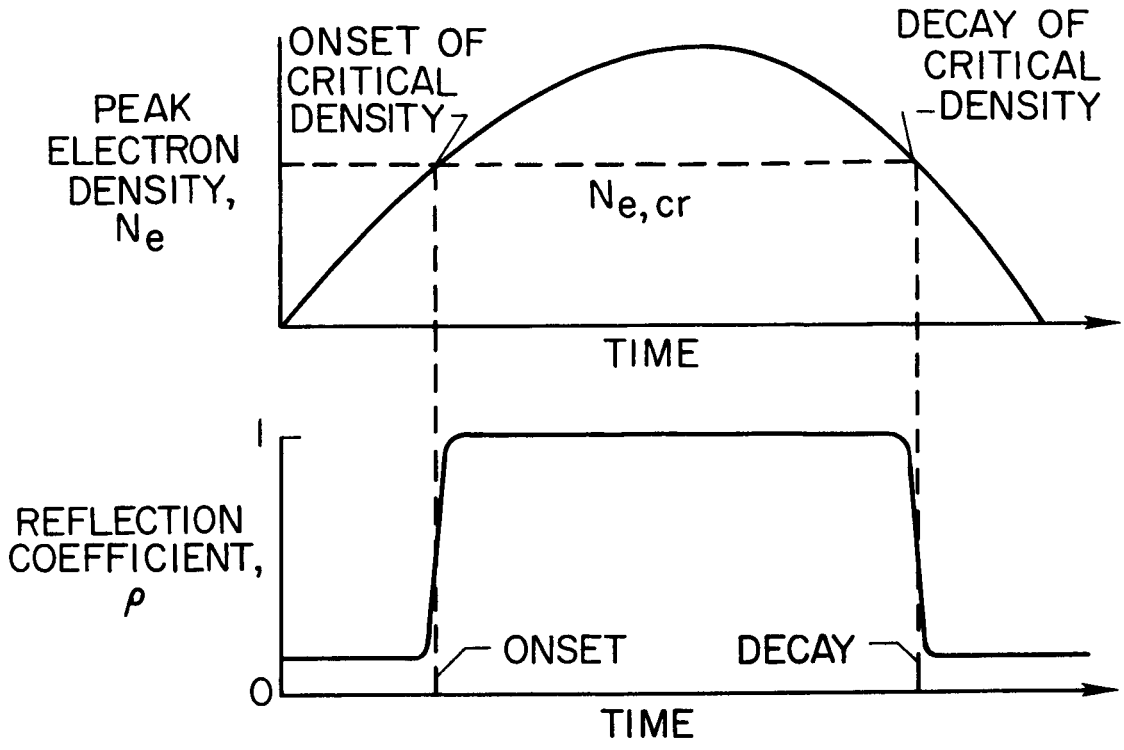

Figure 6.- Application of the reflectometer principle for flight electron density measurements.

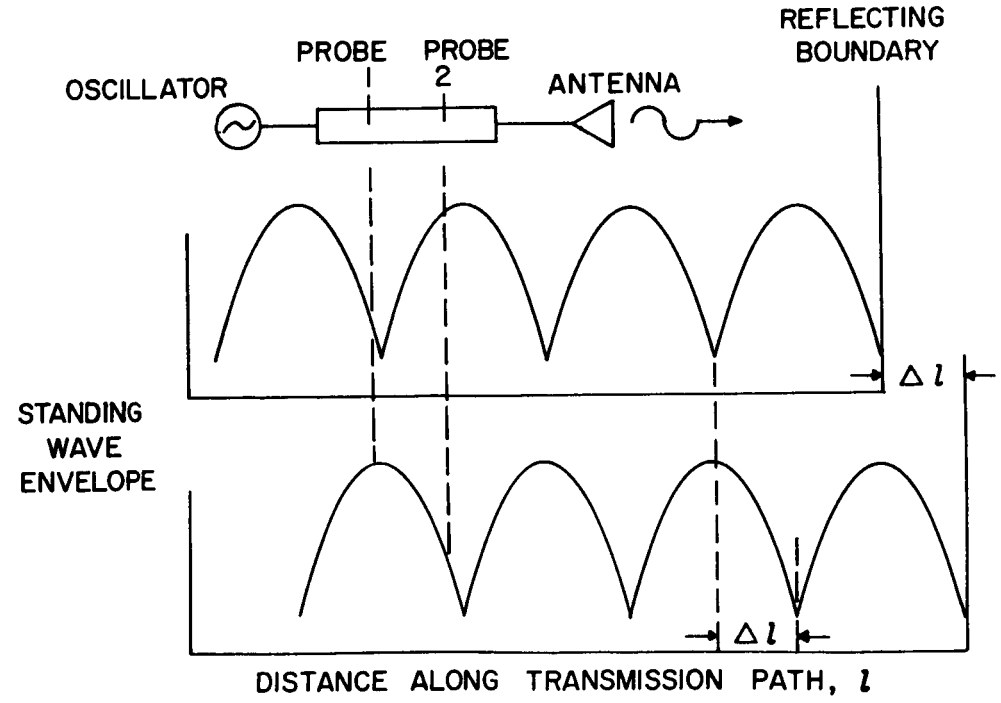

Figure 7.- Measurement of reflecting-boundary standoff distance.

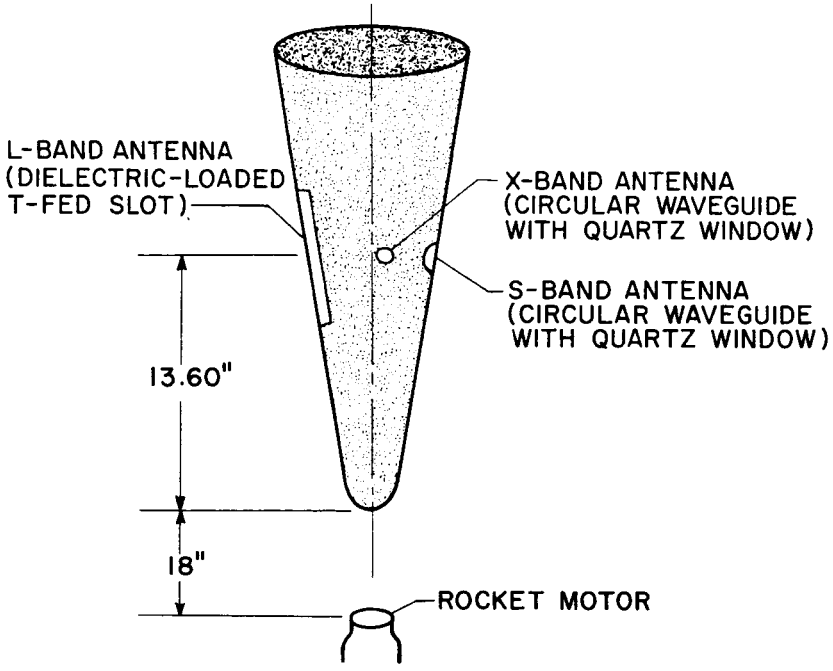

Figure 8.- Reflectometer rocket-exhaust model.

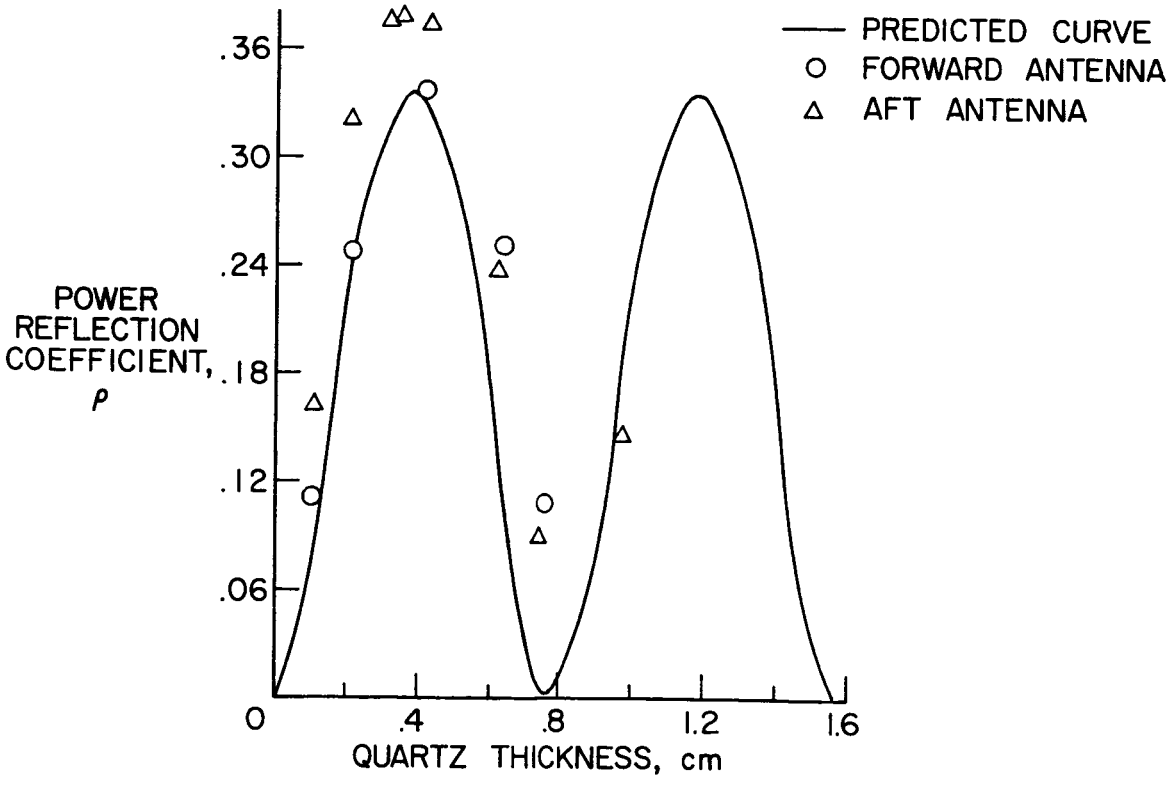

Figure 9.- Typical antenna response to dielectric reflectors. f_3 = 10,044 mc.

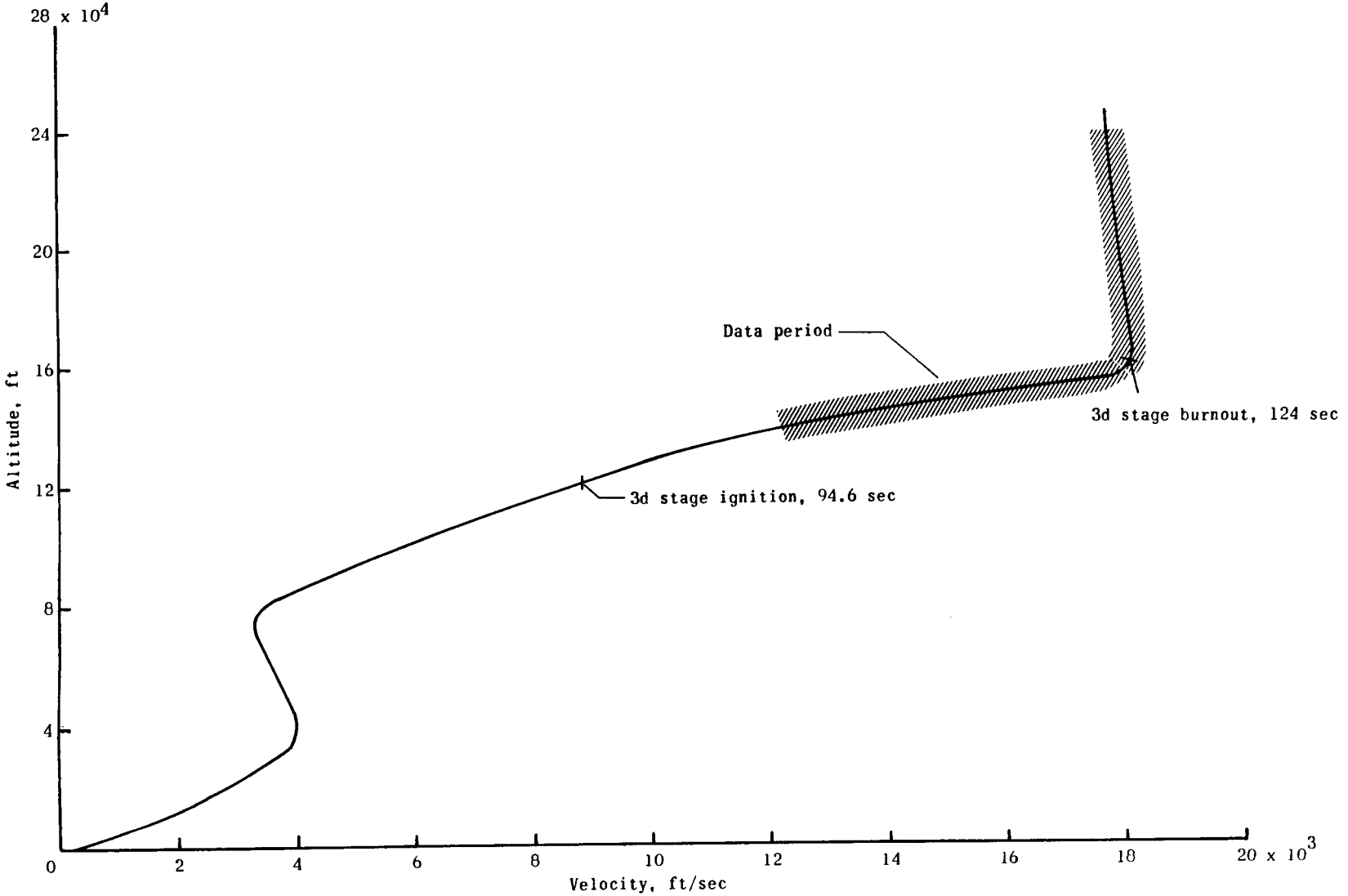

Figure 10.- RAM B3 flight trajectory.

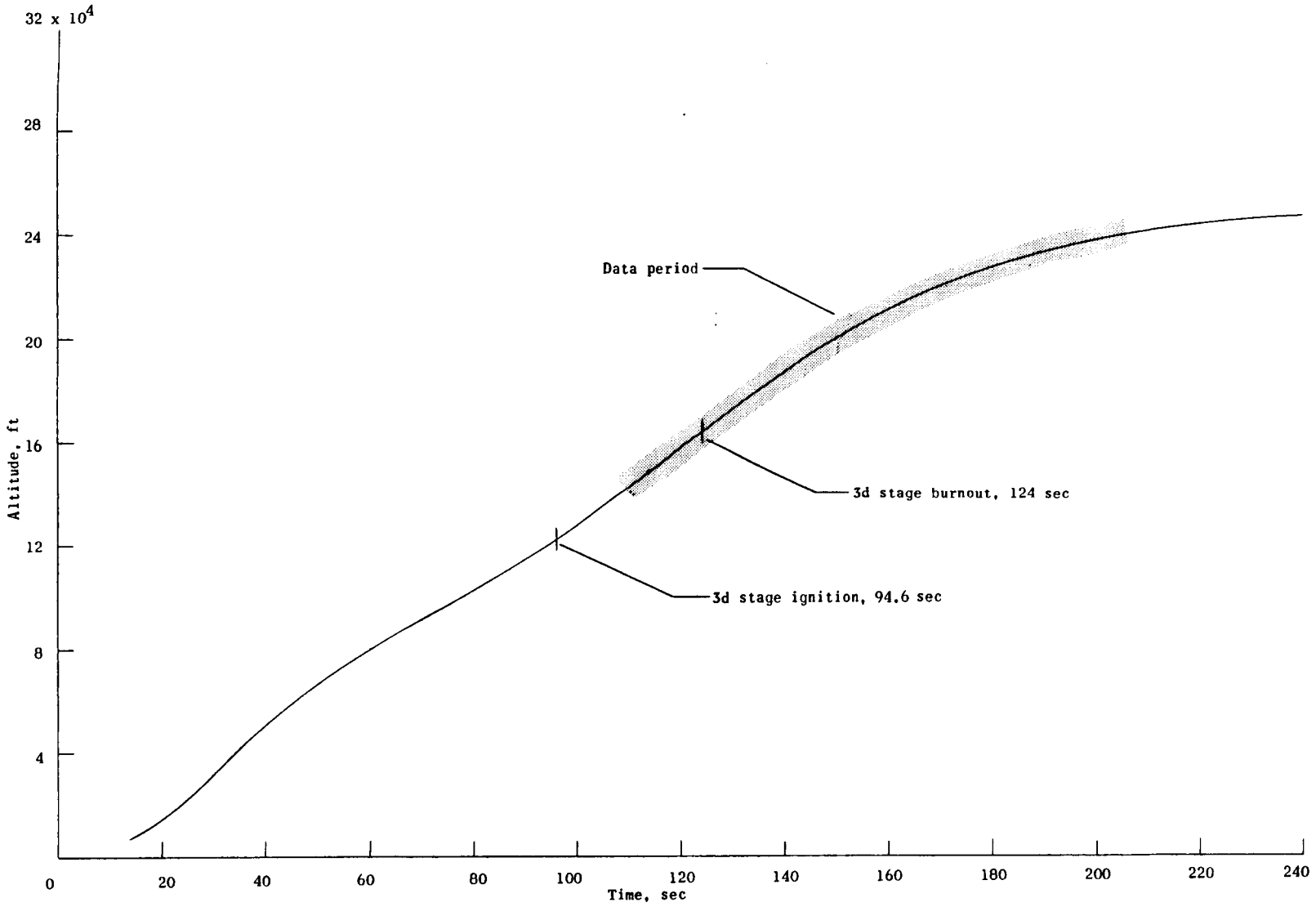

Figure 11.- RAM B3 altitude time history.

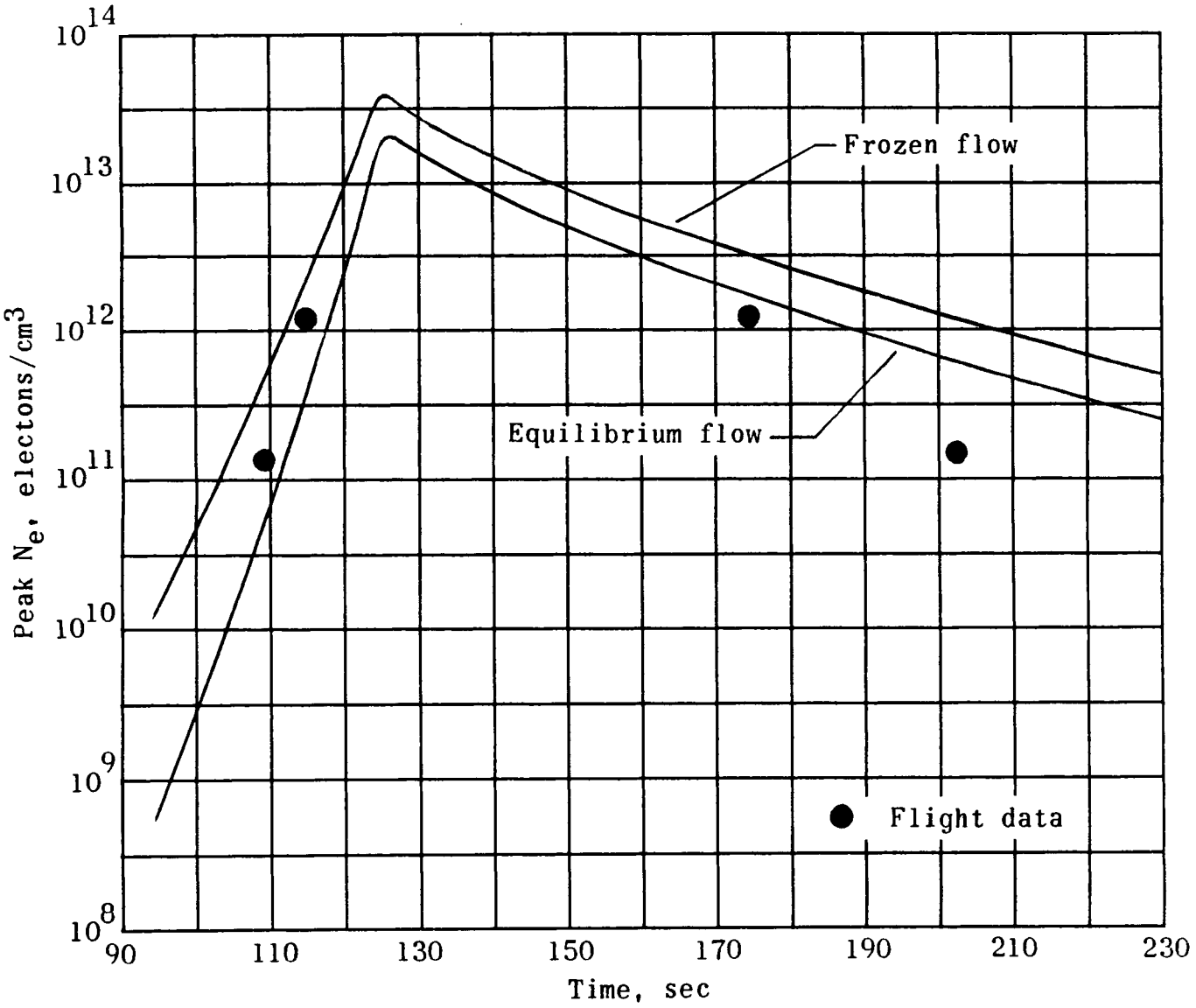

(a) X/D = 0.1475.

Figure 12.- Comparison of measured and calculated electron densities for the RAM flight trajectory.

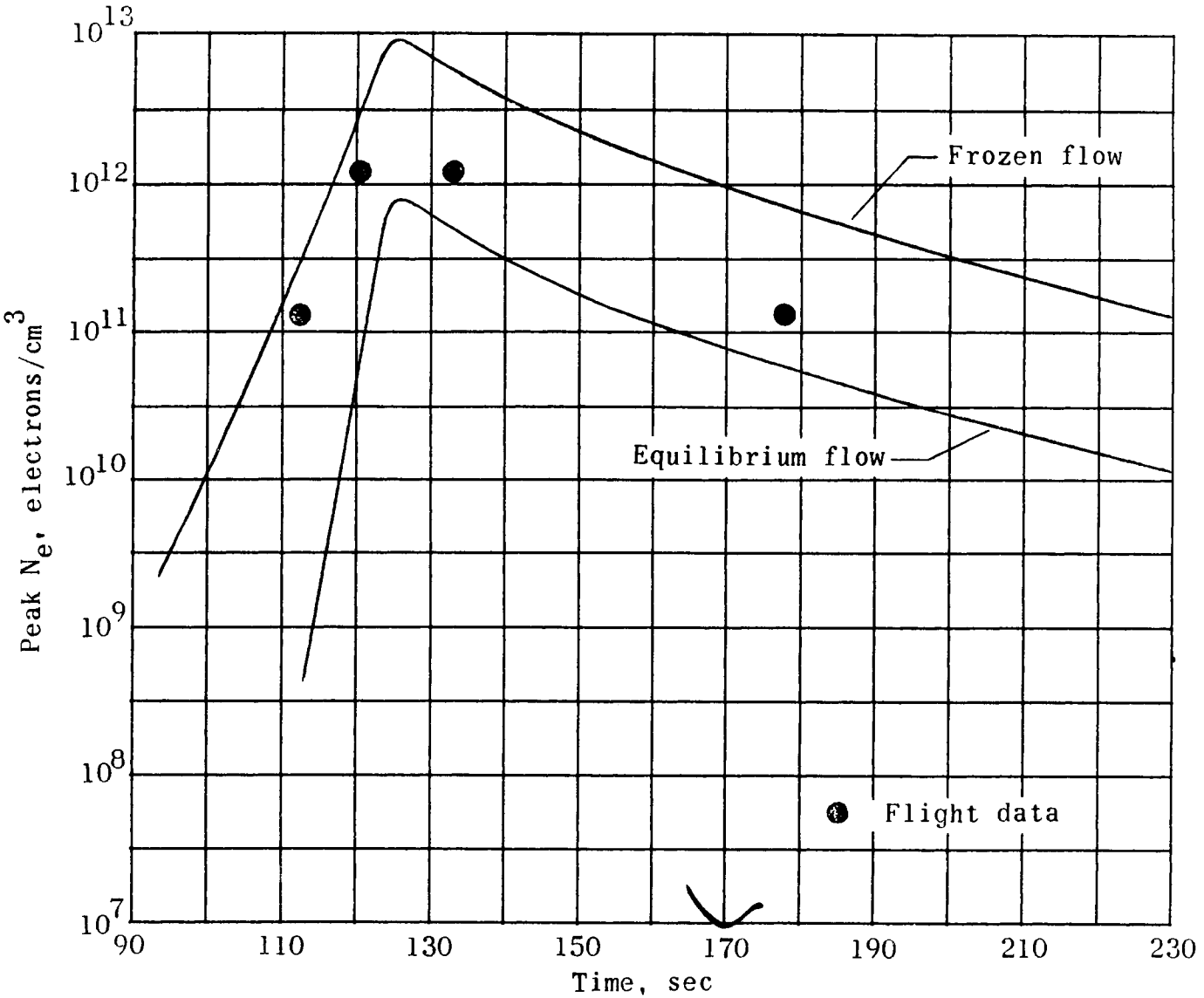

(b) X/D = 0.6.

Figure 12.- Continued.

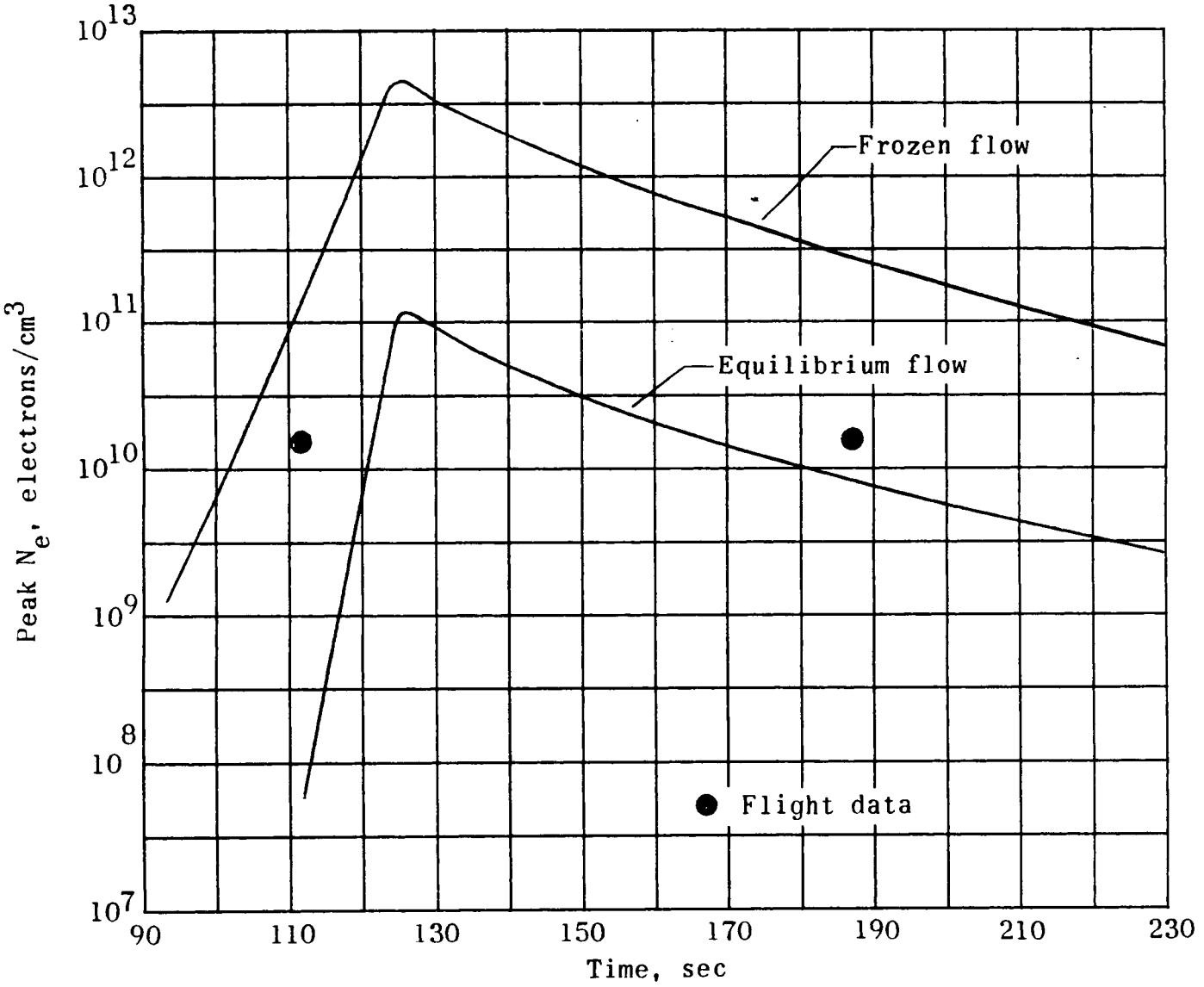

(c) X/D = 3.4.

Figure 12.- Continued.

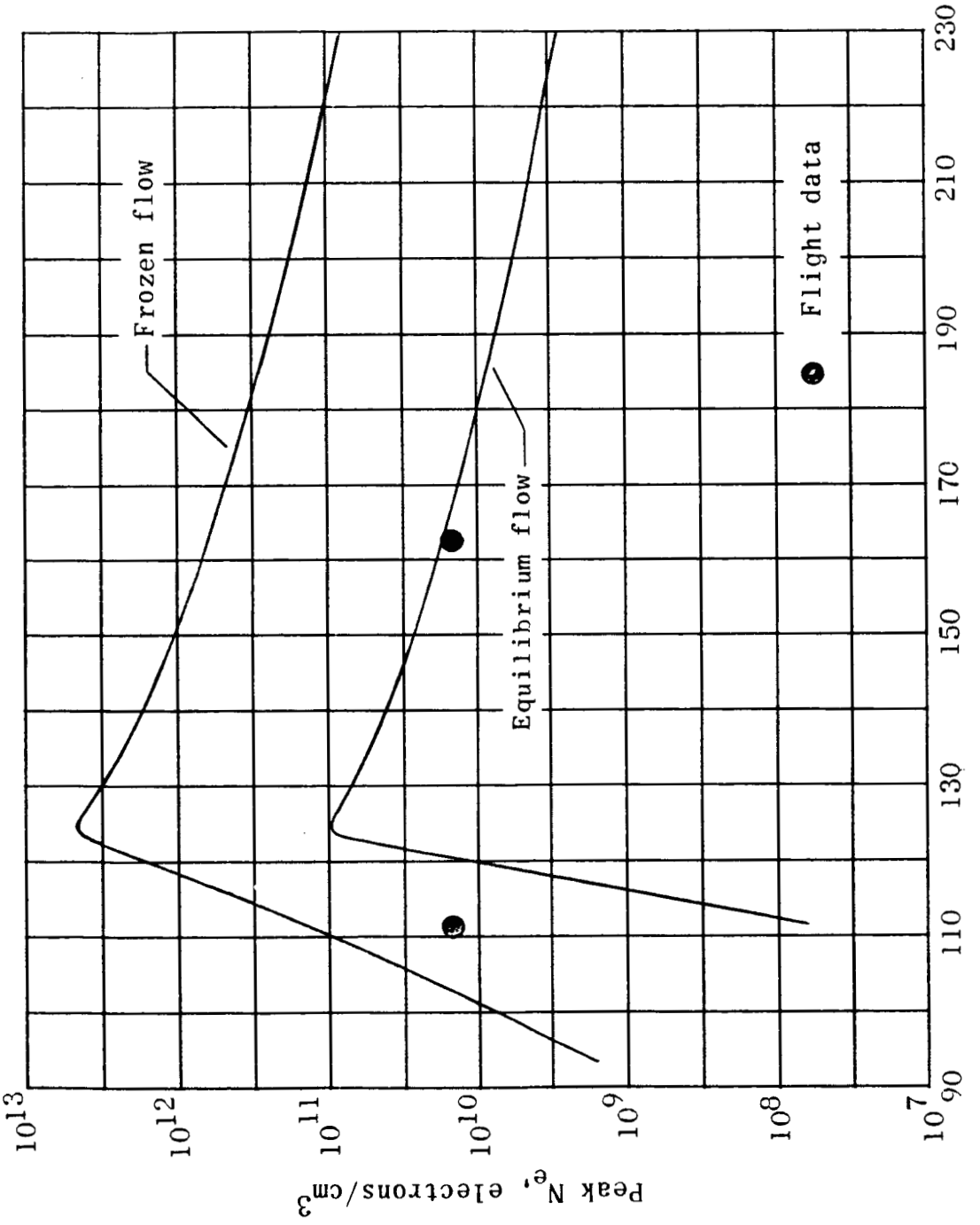

(d) X/D = 4.5.

Figure 12.- Concluded.